

Article

Not peer-reviewed version

Incorporation of Control Parameters Into a Kinetic Model for Decarburization During Basic Oxygen Furnace (BOF) Steelmaking

[Cai Keping](#), [Feng Kai](#)^{*}, [He Dongfeng](#), [Yang Lingzhi](#)^{*}, Zhang Meng

Posted Date: 1 September 2025

doi: 10.20944/preprints202509.0151.v1

Keywords: converter steelmaking; process prediction; kinetic model; decarburization prediction



Preprints.org is a free multidisciplinary platform providing preprint service that is dedicated to making early versions of research outputs permanently available and citable. Preprints posted at Preprints.org appear in Web of Science, Crossref, Google Scholar, Scilit, Europe PMC.

Copyright: This open access article is published under a Creative Commons CC BY 4.0 license, which permit the free download, distribution, and reuse, provided that the author and preprint are cited in any reuse.

Disclaimer/Publisher's Note: The statements, opinions, and data contained in all publications are solely those of the individual author(s) and contributor(s) and not of MDPI and/or the editor(s). MDPI and/or the editor(s) disclaim responsibility for any injury to people or property resulting from any ideas, methods, instructions, or products referred to in the content.

Article

Incorporation of Control Parameters Into a Kinetic Model for Decarburization During Basic Oxygen Furnace (BOF) Steelmaking

Cai Keqing ¹, Feng Kai ^{1,*}, He Dongfeng ¹, Yang Lingzhi ^{2,*} and Zhang Meng ³

¹ School of Metallurgical and Ecological Engineering, University of Science and Technology Beijing, Beijing 100083, China

² School of Minerals Processing and Bioengineering, Central South University, Changsha 410083, China

³ China Metallurgical Industry Planning and Research Institute, Beijing 100013, China

* Correspondence: fengkai-show@163.com (F.K.); yanglingzhi@163.com (Y.L.)

Abstract

Top-bottom combined blowing converter steelmaking involves complex thermodynamic and kinetic processes. The development and application of predictive models for the converter smelting process have long been a focal point in steelmaking research. This paper establishes a kinetic process prediction model for converter steelmaking that can provide on-site guidance. Initially, based on actual production data and real field conditions from a specific company, machine learning models—including BP neural networks, random forests, and XGBoost—are coupled to predict the Tapping Steel Oxygen (TSO) composition for each heat in the production process. The prediction results serve as inputs for the kinetic model. Subsequently, existing kinetic models are analyzed, and an optimized theoretical kinetic model for the converter steelmaking process is selected. The accuracy of this kinetic model is evaluated using measured Tapping Steel Carbon (TSC) data. Finally, a data cyclic iteration algorithm is employed to integrate converter control parameters into the theoretical model of decarburization kinetics. By comparing the prediction accuracy of the decarburization kinetic model before and after incorporating control parameters, the effectiveness of integrating control parameters into the theoretical model is validated. Evaluation results of the decarburization kinetic model's prediction accuracy show that, after incorporating control parameters, the prediction accuracy of TSC carbon content within the range $[-0.2, +0.2]$ improved by 6.26%. This study provides a new approach for optimizing converter kinetic process prediction models and offers significant guidance for real-time monitoring and adjustment in production practice.

Keywords: converter steelmaking; process prediction; kinetic model; decarburization prediction

1. Introduction

During the blowing process of basic oxygen furnace (BOF) steelmaking, it is difficult to obtain accurate and continuous dynamic measurements of key process variables such as temperature and composition changes [1]. As one of the most critical stages in steel production, the core and most challenging aspect of BOF operation lies in the dynamic control of the blowing process. Due to the lack of effective in-process monitoring methods, the current operation often involves a certain degree of blindness and subjectivity, which may lead to excessive top-blowing oxygen supply, resulting in unnecessary consumption of hot metal and other raw materials [2], and consequently increasing energy consumption and production costs. By integrating kinetic theoretical models with actual process control parameters through correction mechanisms, a comprehensive kinetic model for the BOF process can be established. This approach enables a more accurate representation of the internal

evolution during steelmaking, forming the theoretical foundation for soft sensing in the smelting process [3].

To address the prediction challenges in BOF steelmaking, extensive research has been conducted by scholars worldwide. Lin Dong et al. [4] developed a mechanistic model based on the analysis of combined blowing mechanisms and dynamic mass and heat balances during the blowing process, which reflects the variations in steel and slag compositions. Ma Dewen et al. [5] established a BOF prediction model based on the reaction kinetics in the jet impact zone, emulsion zone, and slag-metal interface, aiming to predict the end-point compositions of steel and slag. Dogan N et al. [6] proposed a comprehensive kinetic model for decarburization in oxygen steelmaking based on reaction kinetics. Ik Y et al. [7] developed a process simulation model consisting of a reaction submodel and a scrap melting/dissolution submodel, successfully explaining the redox behaviors of phosphorus and manganese during BOF steelmaking. Although these studies have established relatively mature kinetic and mechanistic models, many model parameters either lack theoretical calculation methods or are inherently unmeasurable, making it difficult to apply them directly in industrial practice.

In this study, selected process control parameters influencing the decarburization reaction are incorporated into the kinetic model, along with optimizable correction parameters. These correction parameters are then optimized using actual production data to enhance model accuracy and facilitate direct operational adjustments in practical BOF operations. The research methodology is as follows: First, existing kinetic models for the decarburization reaction are reviewed and evaluated for their applicability and predictive accuracy in real-world production. A suitable kinetic model capable of integrating control parameters for practical guidance is selected. Using actual plant data, the hit rates for TSC (Tapping Secondary Carbon) and TSO (Tapping Sample Oxygen) predictions are calculated to assess the baseline performance of the original kinetic model. Subsequently, key BOF control parameters are integrated into the kinetic model, and the prediction accuracy is compared before and after the integration to evaluate the improvement. Finally, three machine learning models—Back Propagation (BP) neural network, Random Forest, and XGBoost—are developed to predict the end-point TSO carbon content. These predicted values are used as inputs to the kinetic model, thereby closing the modeling loop and enabling real-time characterization of carbon evolution within the furnace.

2. Prediction of End-Point TSO Carbon Content Using Machine Learning Models

Predicting the end-point carbon content in basic oxygen furnace (BOF) steelmaking is a crucial foundation for achieving stable control of molten steel composition [8]. The Back Propagation (BP) neural network is a multi-layer feedforward neural network based on the error back-propagation algorithm, which exhibits strong nonlinear fitting capability and is therefore suitable for modeling complex, mechanism-unclear processes with intricate variable interactions[9]. The Random Forest model is an ensemble learning method composed of multiple decision trees; it improves prediction stability through voting or averaging strategies and is particularly effective for problems with high-dimensional features, moderate sample sizes, and requirements for model interpretability[10]. XGBoost (Extreme Gradient Boosting) is an optimized algorithm built on the gradient boosting framework, which supports regularization to prevent overfitting and enables parallel computation for enhanced efficiency[11]. In this work, these three data-driven modeling approaches were employed to predict the end-point steel composition in BOF operations, yielding predicted values of the tapping steel oxygen (TSO) carbon content. Subsequently, the predicted TSO results were used as input conditions for a kinetic process prediction model, enabling further optimization and closing the loop of the dynamic process simulation.

2.1. Preprocessing and Feature Selection

The raw data used in this study were collected from actual production records of the entire basic oxygen furnace (BOF) steelmaking process at a steel plant. Input parameters were subjected to data preprocessing to ensure a relatively stable and consistent operational condition. Table 1 presents the statistical summary of the data cleaning process.

Table 1. Statistics of cleaned parameter data.

Governance rules	Original data volume	Cleaned data volume	Cleaning ratio	Remaining data
Duplicate and null value records removed	20400	3208	15.73%	17192
Data Outside reasonable range removed	17192	5693	27.91%	11499

The cleaned process parameters were further constrained within defined screening ranges, as listed in Table 2. Each heat sample is represented by 11 input features: oxygen supply time, total blowing time, oxygen consumption for carbon reduction, hot metal temperature at charging, actual hot metal weight, actual scrap weight, lime addition, lightly burned dolomite addition, pellet addition, dynamic pellet addition, and hot metal carbon content. The output variable is the end-point carbon content of the molten steel at the end of the blow.

Table 2. Reasonable ranges of input parameters (basis for data cleaning).

Input parameters	Maximum value	Minimum value
Oxygen supply time(s)	1018	834
Total blowing time(s)	2850	700
Oxygen consumption for carbon pulling(m³)	11287	9527
Molten iron temperature at charging(°C)	1380	1247
Actual molten iron weight(t)	229.10	203.90
Actual scrap steel weight(t)	29.00	15.80
Lime(kg)	8492	2837
Lightly calcined dolomite(kg)	5132	1439
Pellets(kg)	8592	29
Dynamic pellets(kg)	3070	13
Molten iron-C(w[C])	4.8161	3.9227

After data curation, a dataset comprising 11,499 heats was constructed. Following the empirical rule of splitting the dataset into 80% for training and 20% for testing, the dataset was partitioned into a training set containing 9,199 heats and a test set containing 2,300 heats, as summarized in Table 3.

Table 3. Data distribution after dataset partitioning.

Total dataset size	Training set size	Test set size
11499	9199	2300

2.2. Comparison of Prediction Hit Rates Among the Three Machine Learning Models

The trained BP neural network, random forest, and XGBoost models were applied to the test dataset to predict the end-point TSO carbon content. The prediction errors and accuracy evaluation results are summarized in Tables 4 and 5.

Table 4. Descriptive statistics of prediction residuals from three machine learning models.

Data features	Maximum value	Minimum value	Mean value	Standard deviation	Coefficient of variation
Prediction error of BP neural/%	0.0946	0.0166	0.0471	0.0128	0.2712
Prediction error of random forest/%	0.0287	-0.0487	-0.0021	0.0124	6.0194
Prediction error of XGboost/%	0.0282	-0.0467	-0.0015	0.0125	8.0821

Table 5. Basic prediction accuracy of the three machine learning models.

Carbon content error range/%	[-0.01,+0.01]	[-0.015,+0.015]	[-0.02,+0.02]
Hit rate of BP neural network prediction/%	61.39	89.24	96.43
Hit rate of random forest prediction/%	61.09	90.35	96.63
Hit rate of XGboost prediction/%	60.58	90.30	96.88

From the statistical analysis, it can be observed that the BP neural network performs well within small error ranges, indicating good precision under strict tolerance. However, its improvement in hit rate for larger error ranges is limited, likely due to its tendency to converge to local optima during training. The random forest model demonstrates balanced performance across moderate error ranges and exhibits strong resistance to overfitting, making it suitable for modeling complex nonlinear relationships. In contrast, the XGBoost model shows superior predictive capability across all error levels, particularly excelling under larger tolerance thresholds, highlighting its advantages in both overall accuracy and generalization ability.

2.3. Hybrid Machine Learning Model for Predicting End-Point TSO Carbon Content

Based on the individual prediction accuracies of the three models, a weighted ensemble approach was developed to combine their predictions. Different weights were assigned to each error range to reflect model performance, as shown in Table 6.

Table 6. Weight assignment for four ranges.

Carbon content error range/%	[-0.01,+0.01]	[-0.015,+0.015]	[-0.02,+0.02]
Weight assignment/%	40	30	20

A weighted scoring system was employed to calculate the comprehensive scores for each model: the BP neural network achieved a score of 80.07%, random forest 80.61%, and XGBoost 80.56%. These scores were then normalized to determine the final relative weights: 33.2% for BP, 33.4% for random forest, and 33.4% for XGBoost.

This weight allocation accounts for the performance differences of the three algorithms across various error ranges, ensuring a balanced trade-off between high-precision and moderate-accuracy requirements. By assigning similar yet slightly differentiated weights, the ensemble model fully leverages the strengths of each individual algorithm while effectively mitigating biases that may arise from reliance on a single model.

The final carbon prediction is formulated as: $PC=33.2\%PBP+33.4\%Pforest+33.4\%Pboost$

Subsequently, the predicted TSO carbon content from the hybrid model was used as an input parameter for the kinetic process model. The difference between the predicted and actual measured TSO values was calculated to evaluate the hit rate. The resulting hit rate of the coupled model is presented in Table 7, and the corresponding histogram is shown in Figure 1.

Table 7. Basic prediction accuracy of the three machine learning models.

Carbon content error range/%	[-0.01,+0.01]	[-0.015,+0.015]	[-0.02,+0.02]
Hit rate of TSO prediction after machine learning coupling/%	61.39	91.30	97.88

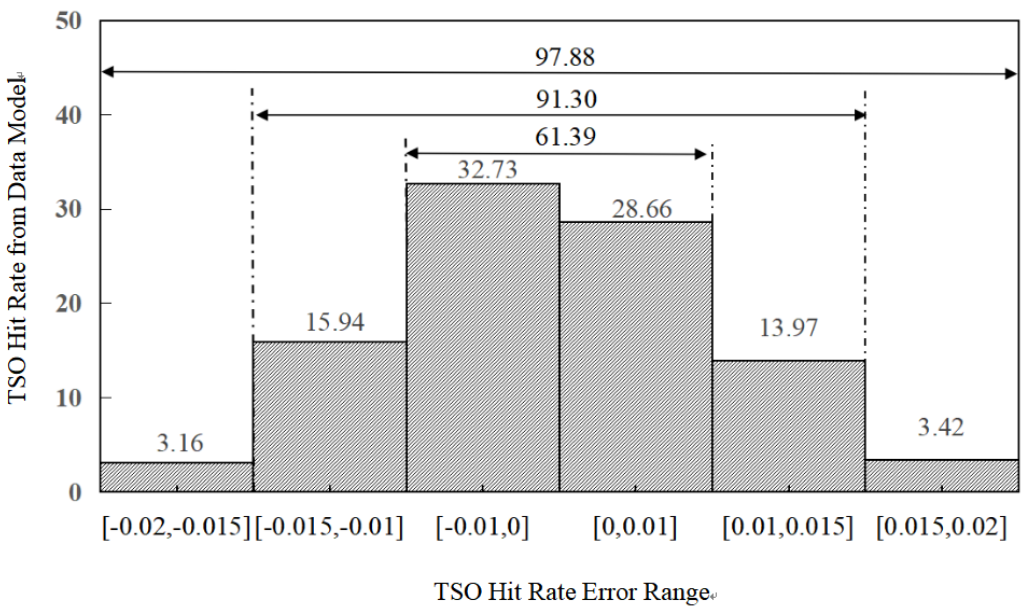


Figure 1. Basic prediction accuracy of the three machine learning models.

Individual models prior to coupling struggle to optimize performance across all error ranges simultaneously, which limits their overall predictive capability. In contrast, the hybrid model demonstrates improved accuracy and stability compared to any single model. It maintains high precision while reducing prediction errors caused by the inherent limitations of individual algorithms. The multi-model fusion strategy not only enhances the robustness of the prediction system but also provides a solid foundation for achieving more precise control in BOF steelmaking processes.

3. Development of a Kinetic Model for Carbon Oxidation during BOF Blowing

Numerous researchers have proposed various kinetic models for the basic oxygen furnace (BOF) steelmaking process to describe and predict the evolution of carbon content during different stages of blowing. Lin Dong [4] focused on analyzing the rate-limiting steps in the decarburization kinetics. Guo Hanjie [12] presented the fundamental principles of the three-stage decarburization process in textbook literature. Cai Wei [13] investigated the decarburization rate in the late blowing period based on Fick’s first law of diffusion. Lin Wenhui [14] classified kinetic models according to measurement methods, distinguishing between sub-lance models and off-gas analysis models. Ma Dewen [5] developed a multi-zone kinetic model that simultaneously describes the behavior of carbon, silicon, manganese, and phosphorus across three distinct reaction zones in the BOF. Table 8 summarizes several representative kinetic models for carbon evolution.

Table 8. Summary of kinetic models for carbon element in converter steelmaking.

Author/ literature	Carbon element kinetic model	Model innovation points	Model accuracy or application
Lin Dong ^[4]	$\frac{d(W_m C_{[C]}^b)}{dt} + \frac{d(EW_m C_{[C]}^b)}{dt} = -\sigma_C(S_m + S_{Em})$	Focus on various limiting factors in kinetics	The calculated carbon mass percentage from the model is in good agreement with the measured values.
GUO Hanjie ^[12]	$-\frac{dC_{[C]}}{d\tau} = k_1\tau$ $-\frac{dC_{[C]}}{d\tau} = k_2$ $-\frac{dC_{[C]}}{d\tau} = k_3(C_{[C]} - C_k)$	Perform kinetic model calculations in stages	Provides the fundamental principles of carbon reaction.
CAI Wei ^[13]	$-\frac{dw_C}{dt} = -D_C \cdot S / \Delta\delta \cdot (w_C - w_C^*)$	Based on Fick's First Law	Studies the decarburization rate in the later stages of the melt pool.
LIN Wenhui ^[14]	$w_{[C]} = w_{[C]}^* + \beta \cdot \ln\{1 + [\exp(\frac{w_{[C]}^{TSC} - w_{[C]}^*}{\beta}) - 1] \cdot \exp[\frac{-10\alpha}{\beta} \cdot \frac{(\Delta V_{Ox} + \sum_i B_i \cdot W_i)}{W_{metal}}]\}$ $v_C = \eta k_1 \cdot [1 - e^{-k_2(w_{[C]} - w_{[C]}^*)}]$	Classify models into sub-lance models and off-gas analysis models based on detection methods	The absolute deviation between the calculated and actual carbon content curves is less than 0.12%.
MA Dewen ^[5]	$-\frac{d[\%C]}{dt} = k_C^z \frac{A_z}{V_m} ([\%C]_z - [\%C]_z^*)$ $\frac{d[\%C]_d}{dt} = \frac{k_d^d A_d \rho_m}{m_d} ([\%C]_d - [\%C]_d^*)$	Regional carbon removal model	The average deviation of the endpoint C mass fraction is within $\pm 0.0058\%$.
ZHANG Qiang ^[15]	$J_C = F_C \{w([C])^b - w([C])^*\} = G_{CO} (P_{CO}^* - 1)$	Study based on coupled reaction mechanisms	The hit rate of the final steel carbon mass fraction within $\pm 0.02\%$ is 89%.
Rout ^[16]	$\frac{dW_C}{dt} = -k_m A_z \frac{\rho_m}{100} \times ([wtpctC]_b - [wtpctC]_{eq})$ $\frac{d[wtpctC]}{dt} = -k_d \frac{A_{app}}{V_{app}} ([wtpctC] - [wtpctC]_{eq})$	Adopt a multi-zone kinetic model with dynamic control parameters introduced	The model predictions were validated against industrial data from Cicutti et al. ^[17] , showing excellent agreement.
Anuththara Kirindigoda Hewage ^[18]	$\frac{dC}{dt} = kA \frac{\rho_m}{W_M} (C_b - C_{eq})$	Apply first-order kinetic models under static and dynamic equilibrium conditions	60% of the heats showed a coefficient of determination(R ²)value above 0.80 for carbon removal.

Existing decarburization kinetic models provide a solid theoretical foundation and technical support for understanding and optimizing the BOF steelmaking process. However, due to the significant challenges in measuring and calculating key parameters at both experimental and theoretical levels, it is particularly important to conduct feasibility analyses by integrating actual operational control parameters[18]. Ma Dewen[5] applied a three-zone kinetic model to simulate the concentration changes of molten metal elements during the blowing process in a 120-ton top-and-bottom combined blowing converter. The model achieved an average prediction deviation of $\pm 0.0058\%$ for the end-point carbon content, validated against actual production data for various steel

grades. Therefore, the decarburization kinetic model proposed by Ma Dewen[5] is selected in this study as the theoretical framework. It serves as the basis for developing a novel approach: by incorporating practical control parameters and iteratively adjusting the model coefficients, we aim to optimize the kinetic sub-models for each reaction zone, thereby enhancing the model's accuracy and adaptability to real-world operations.

3.1. Kinetic Model of the Decarburization Reaction in Basic Oxygen Furnace (BOF) Steelmaking

In current research, the BOF steelmaking process involves reactions occurring across multiple interfaces. The overall reaction kinetics are closely related to interfacial area, residence time, physicochemical properties of the slag, and droplet generation rate. Based on the distinction between the jet impact zone and the emulsion zone, the total decarburization rate can be expressed as [5]:

$$\frac{d(W_m C_{Cm})}{dt} \Big|_{\text{overall}} = \frac{d(W_m C_{Cm})}{dt} \Big|_{iz} + \frac{d(W_m C_{Cm})}{dt} \Big|_{em} \quad (1)$$

where the subscripts iz and em denote the jet impact zone and the emulsion zone, respectively.

3.2. Kinetic Model of the Jet Impact Zone in BOF Decarburization

The oxidation rate of carbon in the jet impact zone can be written as [5]:

$$\frac{d[\%C]}{dt} \Big|_{iz} = -k_c^{iz} \frac{A_{iz}}{V_m} ([\%C]_{iz} - [\%C]_{iz}^*) \quad (2)$$

where: $[\%C]$ is the mass percentage of carbon in the molten steel; A_{iz} is the interfacial reaction area in the jet impact zone (unit: m^2); V_m is the mass of molten steel (unit: kg); k_c^{iz} is the oxygen mass transfer coefficient for carbon in the jet impact zone (unit: m/s).

Furthermore, the oxygen mass transfer coefficient in the jet impact zone can be expressed as follows [5]:

$$k_c^{iz} = 2 \sqrt{\frac{D_c}{\pi} \cdot \frac{(u_1 + 1.16 \times \frac{Qg}{H_{bath}})}{r_{cm}}} \quad (3)$$

where: D_c is the diffusion coefficient of carbon in the metallic droplets (unit: m^2/s); u_1 is the circulation renewal velocity of the molten steel under top-blowing conditions (unit: m/s); Q is the lance gas flow rate (unit: Nm^3/h); g is the acceleration due to gravity (unit: m/s^2); H_{bath} is the bath depth (unit: m); r_{cm} is the impact radius (unit: m).

3.3. Kinetic Model of the Emulsion Zone in BOF Decarburization

In the emulsion zone, the oxidation rate of a single moving metal droplet can be described by a mass transfer-controlled rate equation at the steel side, expressed as follows [5]:

$$\frac{d[\%C]}{dt} \Big|_{em} = -\frac{k_c^d A_d \rho_m}{m_d} ([\%C] - [\%C]^*) \quad (4)$$

where: k_c^d is the mass transfer coefficient of carbon in the emulsion zone (unit: m/s); A_d is the interfacial area of metal droplets in the emulsion (unit: m^2); m_d is the mass of the metal droplets in the emulsion (unit: kg);

The penetration theory can be applied to model the mass transfer coefficient for decarburization of moving metal droplets in the slag-metal emulsion. For spherical droplets rising or falling through the slag layer, the contact time between the metal and slag phases can be approximated as the ratio of droplet diameter to its velocity. The mass transfer coefficient on the steel side can then be calculated as [5]:

$$k_c^d = 2 \sqrt{\frac{D_c u}{\pi d}} \quad (5)$$

where: k_c^d is the mass transfer coefficient of carbon in the emulsion zone (unit: m/s); D_c is the diffusion coefficient of carbon in the metallic droplet (unit: m²/s); u is the velocity of the droplet (unit: m/s); d is the average diameter of the metal droplets (unit: m).

3.4. Prediction Accuracy of the Decarburization Kinetic Theoretical Model

To evaluate the predictive capability of the decarburization kinetic theoretical model for carbon content throughout the entire BOF steelmaking process, an empirical analysis was conducted using actual production data from the enterprise described in Chapter 1. In the kinetic model, the carbon concentration at reaction equilibrium, denoted as [%C]_{eq}, represents the theoretical equilibrium carbon content [19]. However, since the BOF process operates under non-equilibrium conditions and the true equilibrium endpoint is unmeasurable, the measured tapping sample carbon (TSO) content is approximated as the final carbon concentration in the kinetic model.

A random forest-based optimization algorithm was employed to perform global parameter optimization within a search space consisting of 12 key physical and operational parameters, including the average diameter of metal droplets (d_p) and the diffusion coefficient of carbon (DC)[20]. The optimal parameter configuration was achieved by minimizing a weighted mean squared error (MSE) objective function.

The 9,199 cleaned samples from the training set (see Table 3) were used for parameter calibration and model tuning, while the 2,300 samples in the test set were utilized to assess the model's prediction accuracy.

The decarburization kinetic model involves multiple physical parameters, such as the carbon diffusion coefficient (DC) and oxygen lance nozzle radius (r), as listed in Table 9.

Table 9. Parameters of the prediction model for carbon removal kinetics.

Parameter name	Parameter symbol	Unit	Value
Initial carbon mass percentage	C_c^0	%	Actual data for each heat
Final carbon mass percentage	C_c^*	%	Prediction results from coupled data model
Number of nozzles	n	↑	3
Impact radius	r_{cav}	m	0.2
Crater shape angle	θ	°	30
Molten pool depth	h_{im}	m	1
Gravitational acceleration	g	m/s ²	9.8
Oxygen lance radius	r	m	0.1
Droplet area	A_d	um ²	7500
Steel liquid density in emulsion zone	ρ_m	kg/m ³	7000
Average diameter of metal droplets	d_p	um	150
Droplet velocity	u	m/s	0.5
Diffusion coefficient of carbon in metal droplets	D_c	m ² /s	3.5×10 ⁻⁹
Circulation renewal velocity in molten pool under top blowing condition	u_1	m/s	0.1

The predicted TSC (tapping sample carbon before tapping) and TSO carbon contents from the kinetic theoretical model were compared with the corresponding measured values from actual production. The hit rates for TSC and TSO predictions were calculated and are summarized in Tables 10 and 11, respectively. The corresponding histograms are shown in Figures 2 and 3.

Table 10. Precision of TSC carbon content hit rate before introducing control parameters.

Carbon content error range/%	[-0.2,+0.2]	[-0.4,+0.4]	[-0.6,+0.6]
Hit rate of carbon content based on the decarburization kinetics theoretical model(TSC)/%	52.58	88.60	98.89

Table 11. Precision of TSO carbon content hit rate before introducing control parameters.

Carbon content error range/%	[-0.05,+0.05]	[-0.10,+0.10]	[-0.15,+0.15]
Hit rate of carbon content based on the decarburization kinetics theoretical model(TSO)/%	37.54	45.15	52.53

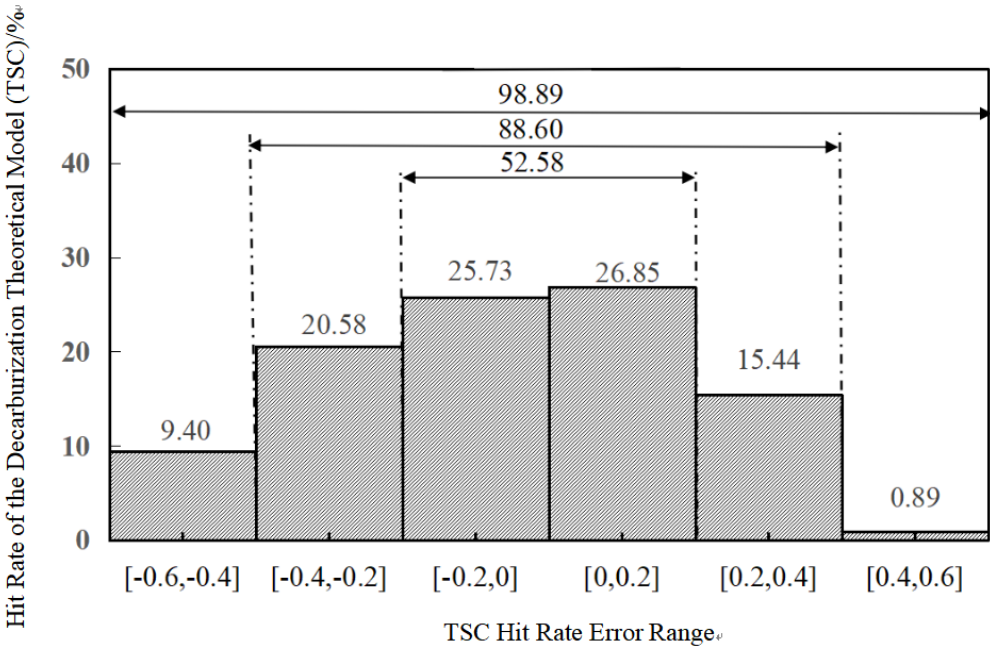


Figure 2. Prediction accuracy of the TSC kinetic model for carbon before optimization.

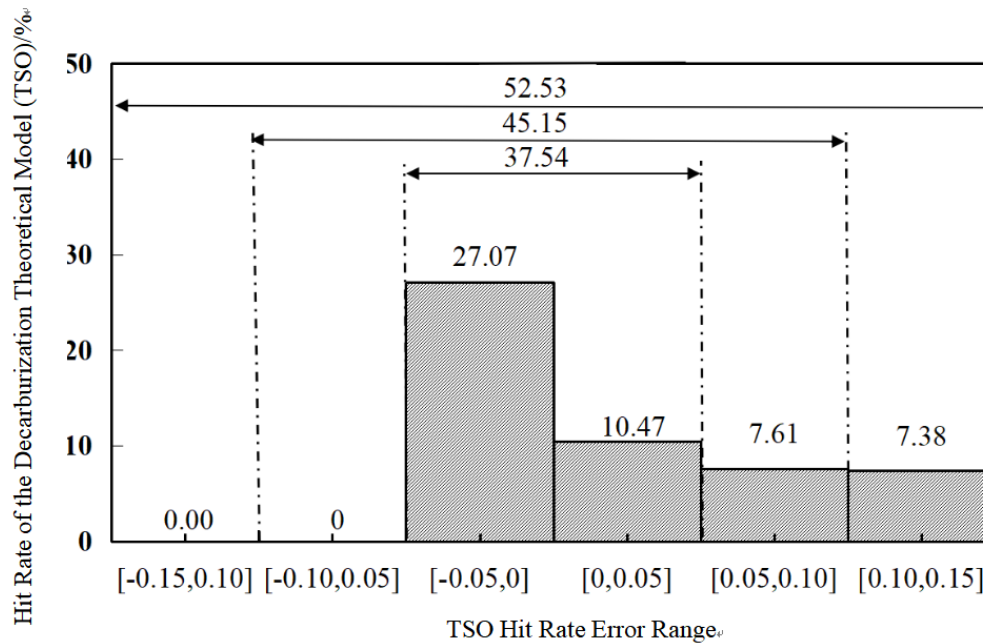


Figure 3. Prediction accuracy of the TSO kinetic model for carbon before optimization.

Analysis of the prediction results reveals that within the error range of $[-0.2\%, +0.2\%]$, only 52.58% of the TSC samples meet this accuracy criterion. Similarly, for TSO carbon content within the narrower range of $[-0.1\%, +0.1\%]$, the hit rate is 52.53%, indicating limited performance at high-precision levels. As observed from the histograms, although a majority of the predicted values are clustered near zero error, a significant proportion of data points exhibit relatively large deviations from the measured values. This suggests that introducing additional influencing variables (e.g., dynamic slag formation, temperature evolution) or refining the calibration of existing parameters could help reduce the gap between predicted and actual carbon content, thereby improving the overall prediction accuracy of the kinetic model.

4. Control-Parameter-Integrated Kinetic Model for Decarburization in the BOF Process

Based on practical operational experience, four key control parameters—lance gas flow rate, lance height, hot metal charge mass, and flux addition amount—are known to significantly influence the mass transfer coefficients in the kinetic reactions of element removal during BOF steelmaking [21]. Therefore, to improve the prediction accuracy of the theoretical decarburization kinetic model and enhance its applicability to real-world production conditions, this study integrates these operational control parameters into the existing two-zone decarburization model. This integration enables the model to better reflect actual process dynamics, effectively avoid abnormal operating conditions and product quality issues, and significantly improve production efficiency [22].

4.1. Revised Kinetic Model for the Jet Impact Zone

Fitting analysis of actual plant data reveals that the hot metal charge mass (M_0) directly affects the physicochemical characteristics of the molten bath—such as temperature distribution and fluid flow behavior—thereby altering the thickness of the mass transfer boundary layer and the diffusion pathways of elements [23]. As M_0 increases, the thermal capacity of the bath rises, leading to changes in jet penetration depth and energy distribution during blowing. To account for this effect, the mass transfer coefficient is dynamically corrected using M_0 . To enhance model robustness [24] and improve its adaptability to variations in raw material inputs, the hot metal mass M_0 is introduced as a scaling factor to quantify the impact of different hot metal batches on mass transfer efficiency. In addition, during actual operation, lance height (h) is frequently adjusted in response to bath level changes and

different blowing stages, significantly influencing the decarburization kinetics. Therefore, incorporating the lance height parameter into the kinetic theoretical model is essential. Operators can use real-time lance height measurements to dynamically update model parameters, enabling adaptive simulation across varying operational conditions[25].

By introducing correction factors for calibration, the revised mass transfer coefficient in the jet impact zone is expressed as:

$$k_c^{iz} = 2e^{bh} \sqrt{\frac{D_c}{\pi} \cdot \frac{(u_l + 1.16 \times \frac{Q \cdot g \cdot M_0^a \cdot k_c^{iz}}{H_{bath}})}{r_{cm}}} \quad (6)$$

where:DC: diffusion coefficient of carbon in metal droplets (unit: m²/s);ul: circulation renewal velocity of molten steel under top-blowing (unit: m/s);Q: lance gas flow rate (unit: Nm³/h);g: gravitational acceleration (unit: m/s²);H_{bath}: bath depth (unit: m);r_{cm}: impact crater radius (unit: m);M₀: hot metal charge mass (unit: kg);a: empirical exponent for hot metal mass correction; k_c^{iz} : calibration coefficient for the jet impact zone;h: lance height above the bath (unit: m);b: empirical constant for lance height adjustment.

4.2. Revised Kinetic Model for the Emulsion Zone

Based on slag-metal reaction thermodynamics and mass transfer principles [26], the lime addition mass (MLime) is introduced as a dynamic correction factor. Lime (CaO), as the primary flux, directly determines the slag basicity (R=CaO/SiO₂) [27], which in turn influences key interfacial properties:

Interfacial tension: Lower interfacial tension enhances wettability and increases the effective slag-metal contact area;

Slag viscosity: Reduced viscosity facilitates mass transfer and element diffusion across phases.

By incorporating MLime into the model, the dynamic impact of flux addition on the mass transfer process can be quantified, thereby addressing the discrepancy between the traditional assumption of constant basicity and the actual operational fluctuations observed in industrial practice [28].

Combining analysis of industrial trial data, a revised mass transfer coefficient model considering the synergistic effect of stirring energy is established:

$$k_c^d = 2 \sqrt{\frac{D_c u M_{Lime}^a}{\pi d}} \quad (7)$$

where: k_c^d : mass transfer coefficient of carbon in the emulsion zone (unit: m/s);DC: diffusion coefficient of carbon in the steel phase (unit: m²/s);u: velocity of metal droplets (unit: m/s);d: average diameter of metal droplets (unit: m);MLime: mass of lime flux added (unit: ton);a: empirical exponent for lime addition, used as a calibration parameter.

4.3. Model Parameter Calibration and Accuracy Evaluation

The predicted end-point TSO from a machine learning-coupled model, along with other kinetic parameters, are used as inputs to the process prediction model. Through continuous comparison with actual BOF operational data, the kinetic model parameters are iteratively optimized and the prediction accuracy is evaluated.

The iterative algorithm is the core of the process simulation, enabling self-adjustment during computation to progressively reduce prediction error. In this study, the forest_minimize function[29] is employed, which uses a random forest-based surrogate model to locate the minimum of the objective function (e.g., weighted mean squared error)[30].

The 9,199 cleaned samples from the training set (see Table 3) are used for parameter optimization of the control-parameter-integrated kinetic model, while the 2,300 samples in the test set are used to assess the final model accuracy.

Through iterative searching, the optimal parameter set that minimizes the prediction error is identified. Combined with the physical parameters listed in Table 9, Table 12 (presented below) summarizes the calibrated control-parameter-integrated kinetic parameters for each reaction zone, obtained through cyclic fitting of the decarburization kinetic model.

Table 12. Control parameters of the decarburization kinetics model fusion.

Parameter name	Parameter symbol	Unit	Value
Exponent of molten iron charge mass	a	Dimensionless	0.75
Coefficient of lance height	b	Dimensionless	0.0005
Correction coefficient of carbon in jet impact zone	k_c^{IZ}	Dimensionless	1.9×10^{-6}

The optimized correction parameters obtained from the parameter tuning process are incorporated into the control-parameter-integrated decarburization kinetic model. Equations (8) and (9) below represent the kinetic models for the jet impact zone and emulsion zone during the BOF steelmaking process, respectively.

$$k_c^{iz} = 2e^{0.0005h} \sqrt{\frac{3.5 \times 10^{-9}}{3.14} \cdot \frac{(0.049 + 1.16 \times \frac{Q \times 9.8 \times M_0^{0.72} \cdot 1.9 \times 10^{-6}}{1.49})}{0.55}}$$

(8)

$$k_c^d = 2 \sqrt{\frac{3.5 \times 10^{-9} \times 570 \times M_{Lime}^{0.75}}{3.14 \times 0.5}}$$

(9)

where: M_0 : hot metal charge mass (unit: t); Q : lance gas flow rate (unit: Nm^3/min); h : lance height above the bath (unit: m); M_{Lime} : mass of flux added (unit: kg).

To evaluate the predictive capability of the control-parameter-integrated kinetic model, the dual-point hit rate at the mid-blowing stage (TSC, Tapping Sample Carbon before tapping) and at the end-point (TSO, final carbon content) is adopted as the core performance metric. The model’s prediction accuracy is systematically analyzed across different error tolerance bands. Taking a real production heat as an example, the following control parameter values are set: Hot metal charge mass: 220 t, Lance height range: 1.5–1.8 m, Lance flow rate: 282 Nm^3/min , Flux addition: 6,500 kg. A comparison of the predicted carbon content (mass%) with and without integrated control parameters is presented in Figure 4, with a close-up view of the mid- and end-point regions shown in Figure 5.

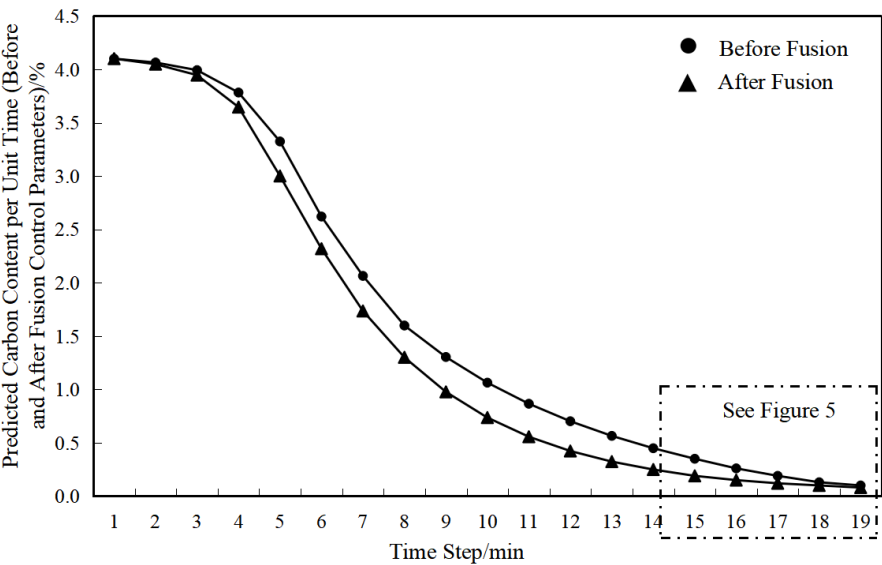


Figure 4. Unit-time predicted carbon content before and after control parameter integration.

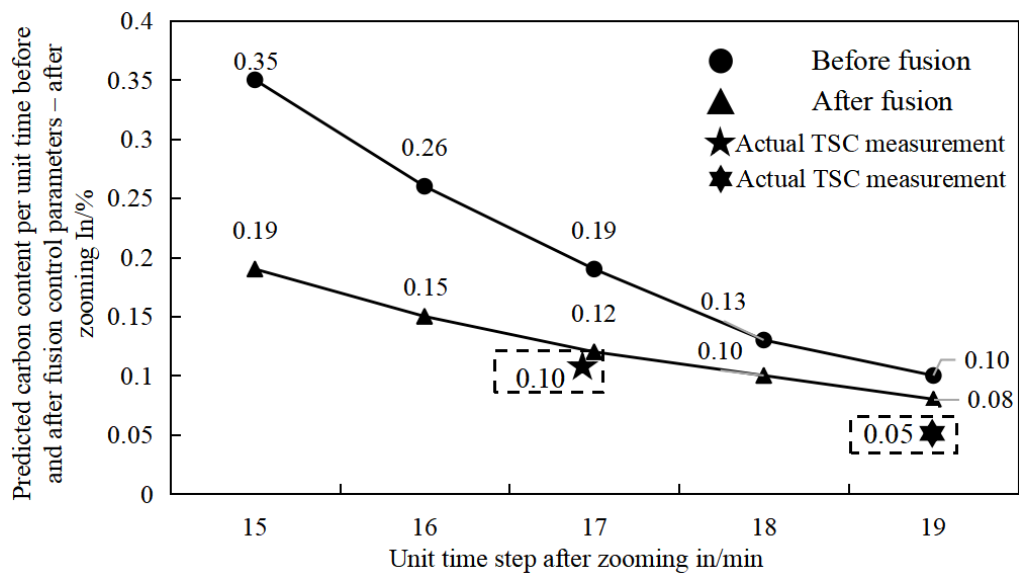


Figure 5. Localized amplification: pre-and post-control parameter carbon content predictions.

At the TSC (mid-blowing carbon measurement) stage, the prediction error of the decarburization kinetic model with integrated control parameters is reduced by 0.07 wt% compared to the model without parameter integration. At the TSO (end-point carbon measurement) stage, the prediction error is reduced by 0.02 wt%. In the complex and dynamic industrial environment, appropriate parameter adjustment helps overcome the limitations of traditional models and provides more reliable predictions.

To evaluate the performance of the optimized model, the predicted TSO and TSC carbon contents from the validation set are compared with actual production data, and the hit rates are calculated based on the absolute deviations. By inputting the actual process parameters for each heat, the hit rates for TSO and TSC before and after optimization are obtained. The comparative results are presented in Figure 6 and Figure 7, respectively.

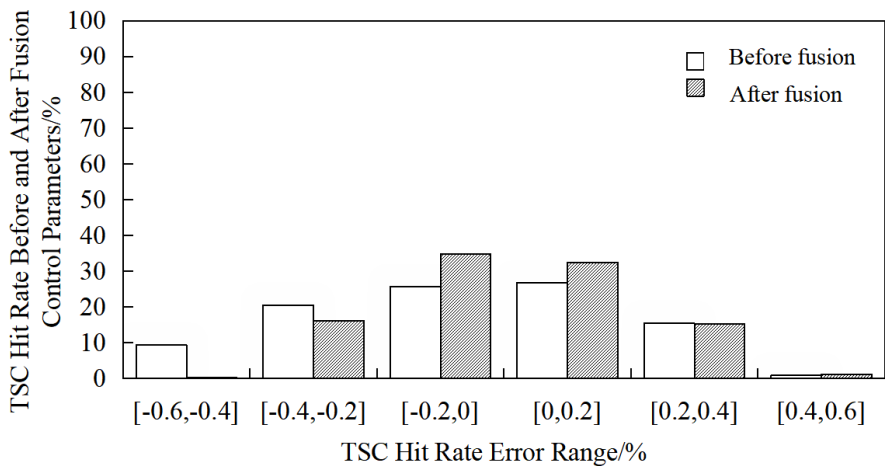


Figure 6. Comparison of prediction for carbon kinetics model(TSC)before and after optimization.

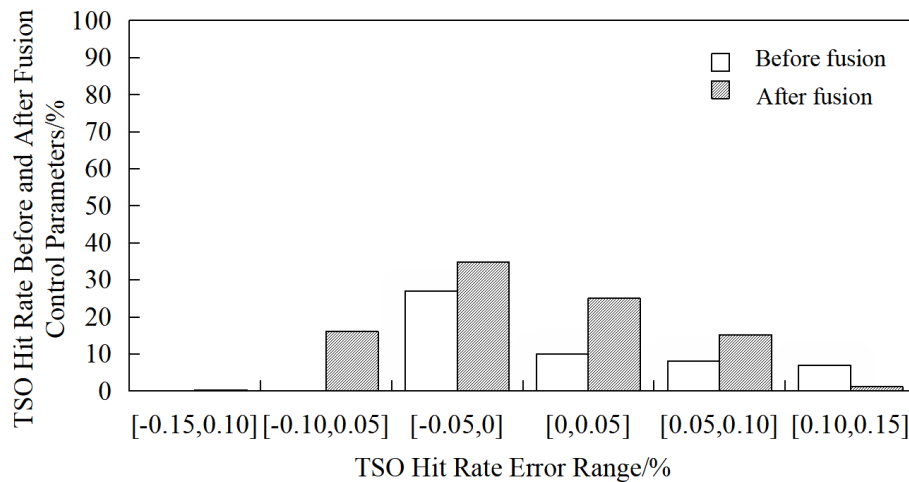


Figure 7. Comparison of prediction for carbon kinetics model(TSO)before and after optimization.

The model achieves a 6.26% improvement in TSC hit rate within the error band of $[-0.2, +0.2]$ wt%, and significant improvements in TSO hit rate: 21.30% increase within $[-0.05, +0.05]$ wt%, 19.51% increase within $[-0.15, +0.15]$ wt%. These results demonstrate the model's enhanced capability in controlling and predicting end-point carbon content. This improvement is attributed to the synergistic optimization of mass transfer coefficients in both the jet impact zone and emulsion zone by the parameter tuning algorithm, particularly through the accurate calibration of the hot metal charge mass exponent and diffusion coefficient.

5. Conclusions

(1) This study presents a novel approach for integrating controllable operational parameters into the theoretical model for decarburization kinetics prediction. For the first time, adjustable parameters such as hot metal charge mass and flux addition amount are deeply coupled with the kinetic model, overcoming the limitations of traditional models that rely on fixed or averaged input parameters.

(2) The end-point carbon content (TSO) is predicted by an ensemble of three machine learning models and used as input to the decarburization kinetic model, replacing conventional equilibrium-based assumptions. This strategy captures heat-to-heat variations and better reflects actual production conditions, enabling a closed-loop optimization of the BOF decarburization kinetic model.

(3) Based on a full year of actual production data from an industrial plant, the proposed model achieves a 6.26% improvement in hit rate for mid-blow carbon (TSC) within the error band of $[-0.2, +0.2]$ wt%, and a 21.30% increase in end-point carbon (TSO) hit rate within $[-0.05, +0.05]$ wt%. These results validate the effectiveness of integrating control parameters in enhancing the accuracy of theoretical decarburization kinetic models.

References

1. CUI B X, LI J, SONG S Y, et al. Quality molten steel control mixing multi-reaction zone dynamics and off-gas analysis system[J]. *Iron & Steel*, 2025, 60(01):84-91.
2. Ghalati, M. K., Zhang, J., Udu, A. G., & Dong, H.. Dynamic Prediction of Reblowing Necessity in BOF Steelmaking. *Proceedings - 2024 International Conference on Machine Learning and Applications*[J]. *ICMLA 2024*:1924-1927.
3. YANG K J. Development of Static and Kinetic Models for Steelmaking in BOF[D]. Northeastern University, 2020(06):20-31.
4. LIN D, ZHAO L C, ZHANG G Y, et al. Mechanism Model Steelmaking Process in Combined Blowing Converter[J]. *China Metallurgy*, 2006, (05):31-35.

5. MA D W,LI J,SONG S Y,et al.Prediction of molten steel composition and temperature based onconverter reaction kinetics[J]. *Steelmaking*, 2023, 39(05):17-26.
6. DOGAN N,BROOKS G A,RHAMDHAN M A.Comprehensive model of oxygen steelmaking Part1:Model development and validation[J].*ISI International*,2011, 51(7):1086.
7. LYTVYNYUK Y, SCHENK J, HIEBLER M,et al. Thermodynamic and kinetic model of the converter steelmaking process:The Description of the BOF model[J]. *Steel Research International* 2014,85:537.
8. LIU Y J,ZHANG X G,PENG Q,et al.Hybrid modeling and multi-network optimization for predictingoxygen supply in converter steelmaking[J].*The Chinese Journal of Process Engineering*,2025,25(05):500-509.
9. XIE L Y,ZHAN D P,LIN Y K,et al.Endpoint Prediction of Converter Steelmaking based onBackpropagation Neural Network[J]. *Journal of University of Science and Technology Liaoning*,2025,27(02):32-36.
10. DONG X X,HAN X,YANG X,et al.A prediction model for dynamic alloy addition after converter based on CNN-LSSVM[J].*Iron & Steel*, 2025, 60(01):75-83.
11. HONG K,ZHAO Z X,ZHONG L C,et al.Development of data driven prediction model for endpoint slagcomposition and slag splashing time of converter[J].*Steelmaking*,2023,39(04):21-27.
12. GUO H J. Metallurgical Physical Chemistry Tutorial [M]. Beijing:Metallurgical Industry Press,2006: 80-102.
13. CAI W.Basic Theory and Application Research on Predictive Model forSteelmaking Process in Combined Blowing Converter[D].China Iron and Steel Research Institute,2024:2-6.
14. LIN W H.Study on Process Behavior Analysis andDecarburizaiton Control of BOF Steelmaking[D].University ofScience and Technology Beijing,2022:10-17.
15. ZHANG Q,YANG Y,DAI Y X,et al.BOF smelting model based on coupling reaction mechanism[J].*Iron & Steel*,,2024,59(08):40-49.
16. Rout, B. K., Brooks, G., Rhamdhani, M. A., Li, Z., Schrama, F. N. H., & Sun, J. Dynamic model of basic oxygen steelmaking process based on multi-zone reaction kinetics: Model derivation and validation.*Metallurgical and Materials Transactions B*[J].*Process Metallurgy and Materials Processing Science*,2018,49(2),537–557.
17. Cicutti C ,Poltarak G ,Ferro S ,.Estimation of Internal Cracking Risk in the Continuous Casting of Round Bars[J].*steel research international*,2017,88(4):20-42.
18. Wang X,Wang Y L,Liu Q G , et al.Energy balance of BOF converter during swirl-type oxygen lance blowing process[J].*Journal of Iron and Steel Research International*,2025,(prepublish):1-13.9
19. Reynoso O A ,Gómez V O ,Calderón R F , et al.Kinetics of austenite formation during continuous heating in as-cast and as-annealed conditions in a low carbon steel[J].*Materials Research Express*,2025,12(2):026502-026502.
20. Zhang H ,Zhong J .Efficient and effective counterfactual explanations for random forests[J].*Expert Systems With Applications*,2025,293128661-128661.
21. Rupesh P ,Murugesan K .A novel two-zone sequential optimization model for pyro-oxidation and reduction reactions in a downdraft gasifier. [J].*RSC advances*,2023,13(14):9128-9141.
22. Hewage K A ,Rout K B ,Brooks G , et al.Analysis of steelmaking kinetics from IMPHOS pilot plant data[J].*Ironmaking & Steelmaking*,2016,43(5):358-370.
23. QIAN Q T,Process Monitoring and Quality Prediction of BasicOxygen Furnace Steelmaking Process Based onFunctional Data Analysis[D].University ofScience and Technology Beijing,2023:5-10.
24. Zhang Y ,Zhu R ,Song X , et al.Distributed operational optimization of multi-energy microgrid clusters considering system robustness[J].*Electric Power Systems Research*,2025,248111990-111990.13
25. Wu C ,Kong Y .Application of Improved Whale Algorithm to Optimize Dephosphorization Process Parameters in Converter Steelmaking[J].*Applied Sciences*,2025,15(8):4277-4277.13
26. Yang Y ,Li L ,Bao J , et al.Numerical simulation on metallurgical transport phenomena during DC casting of large-size Mg-Gd-Y alloy billet under various magnetic fields[J].*Thermal Science and Engineering Progress*,2024,56103082-103082.
27. Zheng K ,Wang W ,Huang T , et al.Influence of temperature and slag composition on wetting behavior of titanium-containing blast furnace slag and tuyere coke[J].*Journal of Iron and Steel Research International*,2025,(prepublish):1-10.

28. Zhang, K., Zheng, Z., Zhang, L., Liu, Y., & Chen, S. Method for Dynamic Prediction of Oxygen Demand in Steelmaking Process Based on BOF Technology. *Processes*, 2023, 11(8):17-30.
29. YANG S C, ZHONG L C, ZHAO Y, et al. Lime Addition Model of Converter based on Random Forest Algorithm[C]. Northeastern University; Jianlong Group, Fushun New Iron & Steel Technology Department, 2022:90-96.
30. LI Q, YANG S Q, CHEN S L, et al. Prediction method of endpoint carbon and temperature of converter steelmaking based on adaptive data augmentation[J]. *Metallurgical Industry Automation*, 2025, 49(02):64-74.

Disclaimer/Publisher's Note: The statements, opinions and data contained in all publications are solely those of the individual author(s) and contributor(s) and not of MDPI and/or the editor(s). MDPI and/or the editor(s) disclaim responsibility for any injury to people or property resulting from any ideas, methods, instructions or products referred to in the content.